

Supporting Information

Performance enhancement of fullerene based solar cells upon NIR laser irradiation

Hardeep Singh Gill^{a, b}, *Sammaiah Thota*^b, *Lian Li*^c, *Akshay Kokil*^b, *Ravi Mosurkal*^c, and *Jayant Kumar*^{a, b*}

^aDepartment of Physics, University of Massachusetts Lowell, Lowell, MA 01854

^bCenter for Advanced Materials, University of Massachusetts Lowell, Lowell, MA 01854

^cU.S. Army Natick Soldier Research, Development & Engineering Center, Natick, MA 01760

*Corresponding author. Tel.: +1 9789343788, Fax: +19784589571.

E-mail: Jayant_Kumar@uml.edu

Spectroscopic measurements:

Glass substrates were cleaned with detergent, acetone and methanol. Thin samples were made by spin-casting the solutions of PCBM and P3HT:PCBM blend on to the cleaned substrates. The spin-coated films on the glass substrates were exposed with the NIR femtosecond laser beam at 800 nm for different time intervals. The laser beam was expanded by a concave lens to completely illuminate the sample. The intensity of the laser beam was controlled to be about 15 mW/cm² using a neutral density filter. As shown in **Fig. S1**, the absorption spectra of the laser exposed thin PCBM films at different intervals of time remained the same as that of the pristine PCBM film. No change to the absorption spectra of the P3HT:PCBM films (**Fig. S2**) upon exposure to the NIR laser pulses was observed.

Morphological Stability Study:

The effect of NIR laser exposure on the morphological behavior of the P3HT:PCBM films under thermal annealing were studied by optical microscopy. The film morphology was examined using a Carl Zeiss Discovery V20 Stereo Microscope equipped with an XYZ stage and CCD camera. P3HT:PCBM thin films (70 nm) with and without the NIR laser treatment were subjected to thermal treatment at 130 °C for 1 h. **Fig. S3** exhibits the impact of laser treatment on the morphology of the films. The non-treated film was homogeneous and free of PCBM micro-crystals. Formation of large PCBM microcrystals was seen in the thermally annealed film. However, the NIR laser exposed and thermally annealed P3HT:PCBM film showed much less PCBM microcrystals and was quite uniform. These observations suggested that the photochemical transformation decreased the thermal diffusion of the PCBM molecules and thereby limited the microcrystal formation. The effect on the nanoscale morphology of the NIR laser exposed and referenced P3HT:PCBM films under thermal annealing were examined by TEM using a Philips EM-400 TEM microscope. For TEM in plain view, the polymer fullerene blend films were floated off from the substrates on water and collected on a copper grid. Bright-field TEM was performed on at an accelerating voltage of 100 kV. These blend films show phase separated structure of bright P3HT rich phase and dark PCBM rich phase. The control annealed P3HT:PCBM film shows large aggregates of PCBM (**Fig. S4 (a)**), while the irradiated P3HT:PCBM film exhibits a homogenous film without any PCBM aggregates (**Fig. S4 (b)**). The domain size of irradiated P3HT:PCBM film is much smaller than that of control P3HT:PCBM film. This observation also supports our findings that the NIR laser irradiation to P3HT:PCBM film suppresses large-scale phase separation of P3HT:PCBM blend and consequently improves the solar cell performance as compared to control cells.

Stability studies of solar cells at high temperatures:

The stability evaluations for the fabricated cells with and without the NIR laser irradiation were also carried out to the fabricated organic solar cells at 80 °C in dark. The key photovoltaic parameters of the

fabricated devices as a function of time are shown in **Fig. S7**. Significant differences between the amount of performance degradation in the laser irradiated cells and the reference cells were observed. For the exposed samples, 88% of J_{sc} , 89% of FF and 95% of V_{oc} were retained after heat treatment at 80 °C for 200 h. The PCE of the exposed samples dropped to 1.15%, maintaining about 74% of its initial value. The control cells stopped working completely after 96 h heat treatment. The enhancement in the stability of the exposed samples could be attributed to the photochemical transformation in the active layer upon exposure to the NIR laser pulses.

MALDI-TOF Measurements:

MALDI-TOF mass spectra of the α -sexithiophene and PCBM samples were acquired. As shown in **Fig. S5**, the mass spectra of α -sexithiophene remained the same after exposure to the NIR laser irradiation. The mass spectra of the NIR laser irradiation treated and non-treated PCBM samples are illustrated in **Fig. S6** and **Table S1**. The mass spectrum of the laser exposed sample showed a peak at m/z 1440 ($M^+ - 380$) which can be ascribed to a major fragmentation peak of the dimerized PCBM monomers that occurred at the conjunction of the C_{60} cage and phenyl-butyric acid methyl ester side chain (**Table S1**).

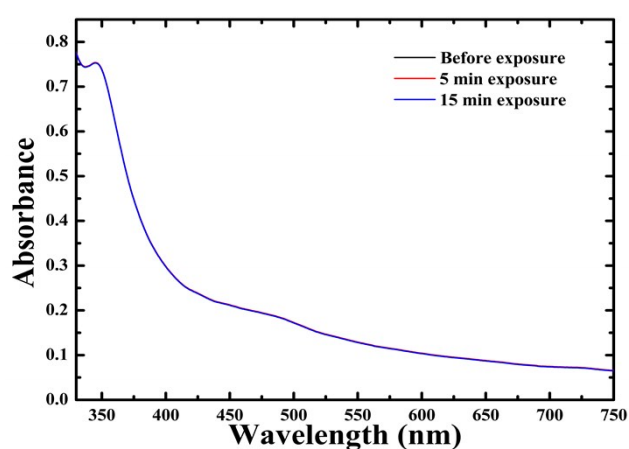


Fig. S1. UV-vis absorption spectra of a pristine PCBM film, and the same PCBM film after 5 min and 15 min exposure to the NIR laser pulses.

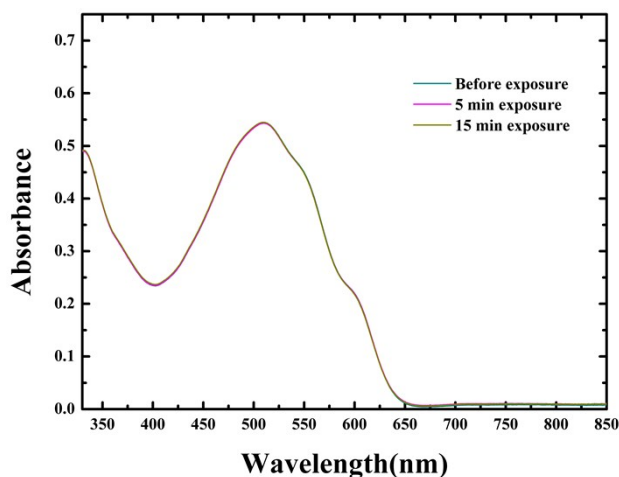


Fig. S2. UV-vis absorption spectra of a P3HT:PCBM film with and without 5 min and 15 min NIR laser exposure .

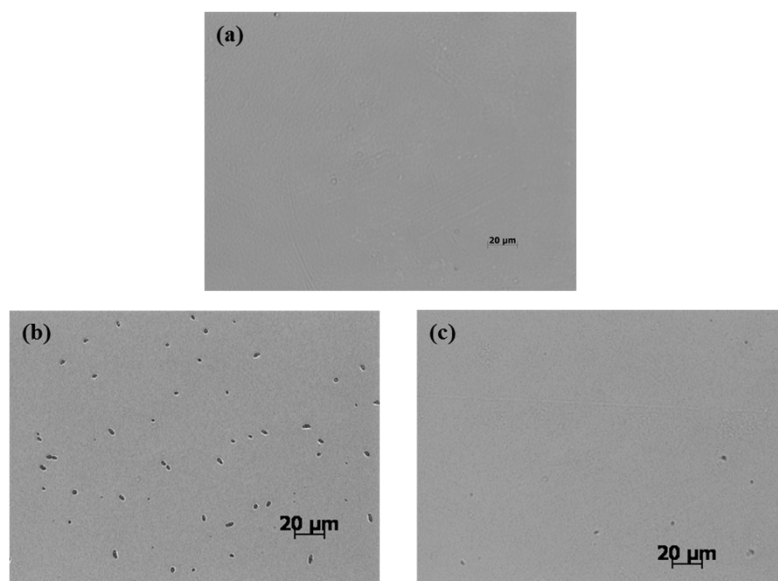


Fig. S3 Optical microscopic images of (a) a P3HT:PCBM film coated on glass substrate, (b) a P3HT:PCBM film after 1 h of thermal annealing at 130 °C and (c) a P3HT:PCBM film after 15 minutes NIR laser exposure and 1 h of thermal annealing at 130 °C.

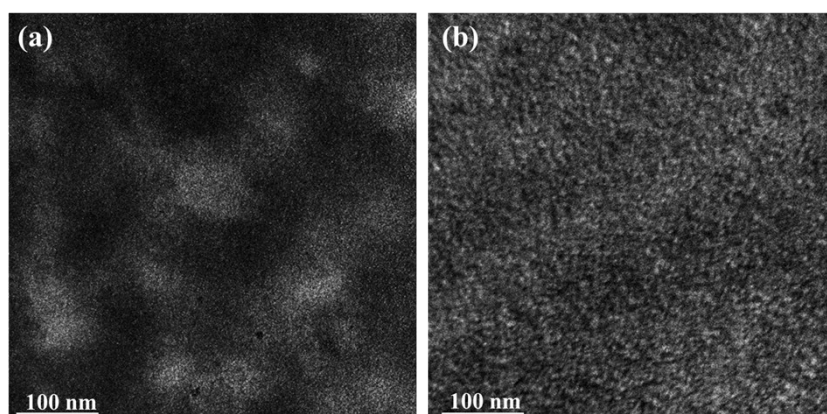


Fig. S4 Comparison of TEM images of (a) the P3HT:PCBM film after 1 h of thermal annealing at 130 °C and (b) a P3HT:PCBM film after 15 minutes NIR laser exposure and 1 h of thermal annealing at 130 °C.

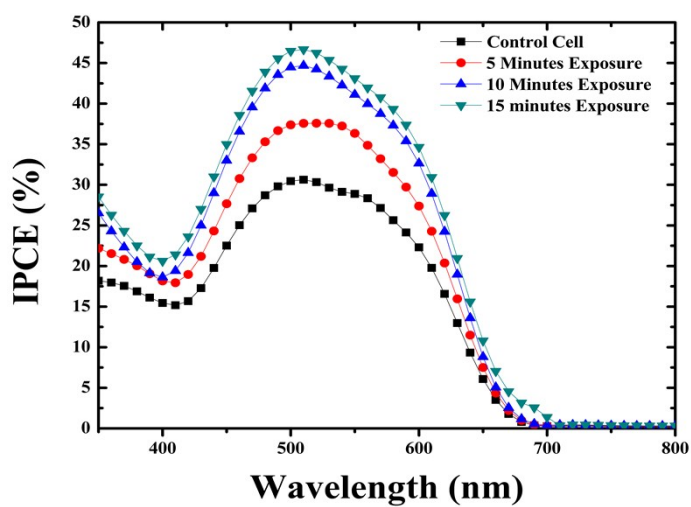


Fig. S5 IPCE spectra of the BHJ-OSCs without (filled squares) and with 5 min (filled circles), 10 min (filled triangles), and 15 min (filled inverted triangles) exposure to NIR laser pulses.

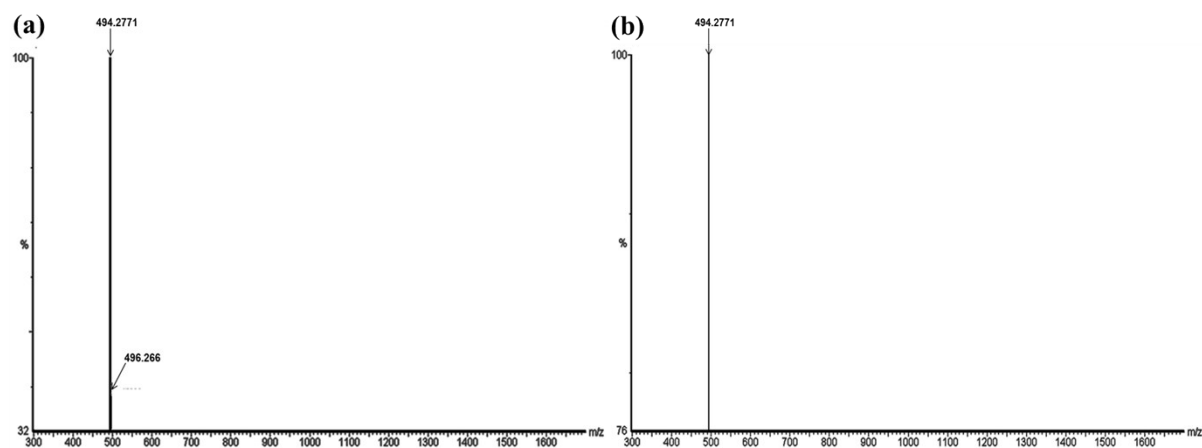


Fig. S6 MALDI-TOF mass spectra of (a) an α -sexithiophene sample and (b) an α -sexithiophene sample after exposure to NIR laser irradiation for 15 min.

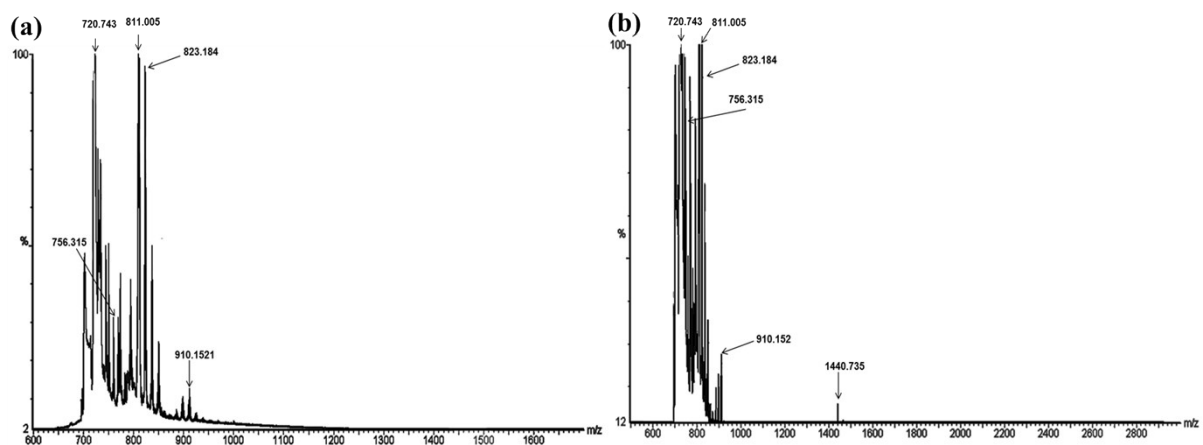


Fig. S7 MALDI-TOF mass spectra of (a) a PCBM sample and (b) a PCBM sample after 15 min NIR laser exposure.

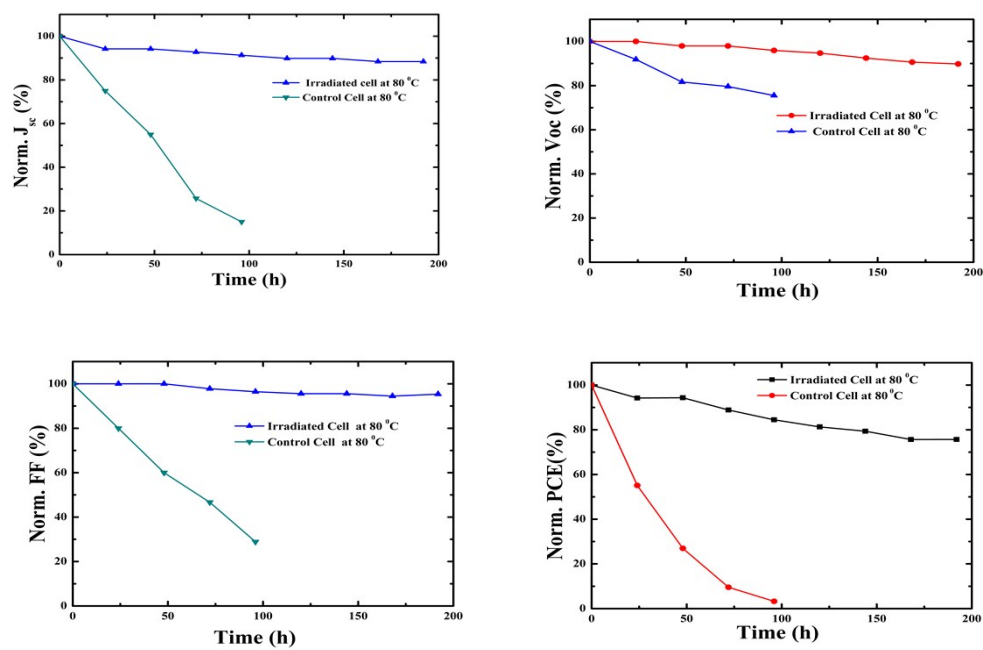
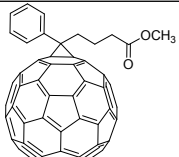
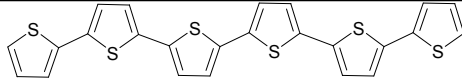
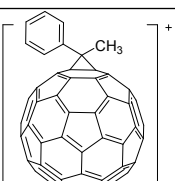
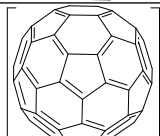
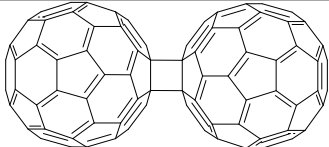
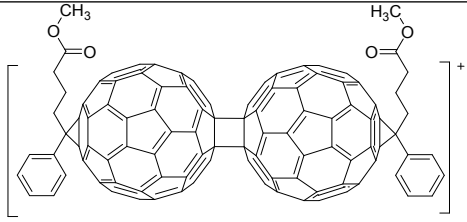


Fig. S8. Stability evaluation of the key photovoltaic parameters of the 15 min NIR laser exposed solar cells as compared to the control cell at 80°C.

Table S1. Structural assignment of peaks observed in MALDI-TOF mass spectra.

Chemical Structures	Theoretical (m/z)	Observed MALDI-TOF (m/z)
	910	910.52
	494	494.246
	823	823.165
	720 6	720.743

	1440	1440.735
	1820	